A&A 520, A89 (2010)
DOI: 10.1051/0004-6361/200913796

Astronomy & Astrophysics

Physical elements of the eclipsing binary δ Orionis⋆,⋆⋆,⋆⋆⋆

P. Mayer[1], P. Harmanec[1], M. Wolf[1], H. Božić[2], and M. Šlechta[3]

[1] Astronomical Institute of the Charles University, Faculty of Mathematics and Physics, V Holešovičkách 2, 180 00 Praha 8, Czech Republic
e-mail: mayer@cesnet.cz
[2] Hvar Observatory, Faculty of Geodesy, Zagreb University, Kacićeva 26, 10000 Zagreb, Croatia
[3] Astronomical Institute, Academy of Sciences of the Czech Republic, 251 65 Ondřejov, Czech Republic

Received 3 December 2009 / Accepted 1 June 2010

ABSTRACT

For years, δ Orionis was considered a normal binary with an O9.5 II primary exhibiting apsidal-line advance. However, radial-velocity curves of both binary components have been derived from the IUE and optical spectra using the cross-correlation technique, and surprisingly low masses of 11.2 and 5.6 $M_\odot$ were found. We obtained new spectra in the red spectral region and new UBV photometry. Using all published photometry and radial velocities, we deduced more accurate orbital and apsidal line periods. The main result of this paper is to show that the observed line spectra of δ Orionis are composed of the lines of the O9.5 II primary and a similarly hot tertiary, while the lines of a cooler B-type secondary are too faint to be detected in the available spectra. The character of the light curve (low-amplitude partial eclipses and a non-negligible scatter of the data) does not allow for a unique light-curve solution. Nevertheless, we show that the assumption of normal primary-component mass and radius corresponding to the O9.5 II classification (25 $M_\odot$, 16–17 $R_\odot$) leads to consistent parameters for the system.

Key words. binaries: eclipsing – stars: early-type – stars: fundamental parameters – stars: individual: δ Ori

1. Introduction

The star δ Orionis A (HR 1852, HD 36486, HIP 25930) is one of the brightest eclipsing binaries on the sky. It has an orbital period of $5\overset{\mathrm{d}}{.}732$, the primary star is of spectral type O 9.5 II (Walborn 1972), visual magnitude of the system is $2\overset{\mathrm{m}}{.}20$ at maximum, and depths of minima are $0\overset{\mathrm{m}}{.}11$ and $0\overset{\mathrm{m}}{.}07$ for the primary and secondary, respectively. The eclipsing binary is a member of the multiple visual star ADS 4134. Besides the somewhat faint and distant components B and C, there is a close component Ab discovered by Heintz (1980) and confirmed by speckle interferometry (Mason et al. 1999) and by *Hipparcos* satellite (Perryman & ESA 1997). The last source gives the separation between Aa and Ab as $0\overset{''}{.}267$ and their magnitude difference $1\overset{\mathrm{m}}{.}35$ (probably the average difference during the orbit). Horch et al. (2001) give the magnitude difference $1\overset{\mathrm{m}}{.}59$. A preliminary astrometric orbit with a period of 201 years has been published by Mason et al. (2009). They give the magnitude difference $1\overset{\mathrm{m}}{.}4$, which will be used hereafter.

The binary has been studied many times. The first four radial velocities (RV) were published by Vogel & Scheiner (1892), and the RV variability was discovered by Deslandres (1900a, b) and confirmed by Campbell (1901). Deslandres (1900a) analysed 11 Meudon RVs and concluded that δ Orionis is a spectroscopic binary with a period of $1\overset{\mathrm{d}}{.}92$ and a highly eccentric orbit. Hartmann (1904) obtained and analysed Potsdam RVs, including the remeasured early RVs of Vogel & Scheiner (1892). He found that the correct orbital period, also reconciling Deslandres' and Campbell's RVs is $5\overset{\mathrm{d}}{.}7325 \pm 0\overset{\mathrm{d}}{.}0002$. A number of studies followed. These were summarized by Harvey et al. (1987) who derived new RVs from the International Ultraviolet Explorer (IUE) SWP spectra. After analysing published and new RVs they got a sidereal period of $5\overset{\mathrm{d}}{.}732403$, the eccentricity $e = 0.087$, and the period of the apsidal-line rotation of 225 ± 27 years. Also the value of $K_{\mathrm{pri}} \approx 100$ km s^{-1} appeared well established. Luyten et al. (1939) gave the mass ratio 2.6, and with it, Koch & Hrivnak (1981) obtained quite acceptable masses: 23 and 9 $M_\odot$.

Owing to its brightness, this binary could be a welcome source of precise physical properties of early-type stars; but the presence of the visual component and the low depths of minima (and probably also some intrinsic variability) make the exploitation of observations rather difficult. In a recent study, Harvin et al. (2002; hereafter H02) published new values of masses and other parameters of the binary components (also discussed by Harvin & Gies 2002). They found quite surprising masses for the system components: $M_1 = 11.2$ and $M_2 = 5.6\,M_\odot$. These values followed from the radial-velocity (RV hereafter) curve semi-amplitudes obtained using 60 high-dispersion IUE spectra and also a set of ground-based spectra, which consisted of 6 KPNO and 14 Mount Stromlo Observatory spectra, all with resolution $\lambda/\Delta\lambda 14\,000$ to 32 000 and an S/N of 200 to 300 pixel^{-1}. To obtain RVs, H02 used the cross-correlation function (CCF). The inclination of the orbit was found from the solution of the light curve obtained by *Hipparcos*.

One would expect a considerably higher mass for the primary component, perhaps not as high as expected by H02 (26–30 $M_\odot$), but certainly above 20 $M_\odot$; e.g., in Schmidt-Kaler (1982) the value 22 $M_\odot$ can be interpolated for the given spectral type and luminosity. Heap et al. (2006) give such a value for

⋆ Based on new spectral and photometric observations from the Hvar and Ondřejov observatories.

⋆⋆ Tables 1 and 2 are only available in electronic form at the CDS via anonymous ftp to cdsarc.u-strasbg.fr (130.79.128.5) or via http://cdsarc.u-strasbg.fr/viz-bin/qcat?J/A+A/520/A89

⋆⋆⋆ Appendix A is only available in electronic form at http://www.aanda.org

the O 9.7 III star. The low masses of components obtained by H02 are difficult to explain; since the orbit is eccentric, it seems probable that there was no strong interaction between the primary and secondary in the previous history of the binary, and both components should have been evolving as single stars.

In Sect. 5, it is shown that, although the primary component is evolved to a radius well over MS, it is safely inside its Roche lobe. We compared the δ Orionis spectra with synthetic spectra (CMFGEN – Hillier & Miller 1998, OSTAR – Lanz & Hubeny 2003, BSTAR – Lanz & Hubeny 2007) and found no indications that the components (namely, the primary one) possess any abnormalities as might be the case for very low masses. The IR excess noted by H02 is only modest. Therefore, some doubts about the H02 results are natural.

In several cases, unexpected masses of certain binaries were ultimately explained by the presence of the spectral lines of a third body. Since δ Orionis is also a triple system, the strange masses found by H02 can perhaps be also due to inappropriate treatment of the contribution of the third body to the observed line profiles.

The problem can lie in the application of the CCF method to the IUE spectra with their relatively low S/N. It is surprising – as H02 themselves admit – that no trace of the visual companion was found in the IUE spectra. This companion should perhaps contribute more light in UV than in visual (using $1\overset{\mathrm{m}}{.}4$ mag difference, $L_{V,3} = 0.216$; $L_1+L_2+L_3 = 1$) since there are reasons to expect that its temperature is higher than the temperature of the primary, see Sect. 6. Very probably, the irregular and ill-defined CCF as shown in Fig. 3 of H02 is the reason; the line of the third body that is very wide (see Sect. 4) might go unnoticed there.

That the third line was not recognized in the IUE spectra was the reason the secondary line was "found". The complicated process used by H02 to separate this line from the CCF profile does not appear as convincing. The results can be explained equally well as the effect of the third line. The red and blue extensions of this wide line might be misinterpreted as "secondary lines". This is particularly notable in the lower part of Fig. 4 of H02, where the dark areas have the form of straight lines and not of a sine curve. We show in Sect. 4 that the true lines of the secondary are much weaker than those found by H02.

In the H02 study, δ Orionis is compared with δ Cir and LZ Cep, where masses lower than expected were found as well. In both these binaries, the mass deviation is only modest, and the mass determination is not without problems, especially due to the uncertain inclinations. Since δ Cir is also a triple star and was analysed with the CCF (Penny et al. 2001), determination of its component masses could be affected in a similar way to the case of δ Ori. On the other hand, LZ Cep is a *semi-detached* binary (Harries et al. 1998), therefore its component masses should differ from normal ones.

2. Observational material used

We compiled all published RVs with known times of observations, accumulated since 1888, and derived HJDs for them. We also reduced 20 Reticon and 204 CCD spectrograms obtained in the coudé spectrograph of the Ondřejov 2.0-m reflector between 1993 and 2010. Details on the reduction and measurements of the new spectra and compilation of published RVs can be found in Appendix A. All individual RVs with HJDs are provided for future use in electronic-only Table 1.

We obtained new *UBV* observations at Hvar and also compiled available observations with known dates of observations. A detailed account of these data, their reduction and homogenization is in Appendix B. For the convenience of future investigators, we publish both the new and all the available photoelectric observations homogenized by us in electronic-only Table 2. The orbital phase plots for all numerous enough data sets, which were obtained in the visual spectral region are shown in Fig. 1. One can see that neither light curve is ideal for the determination of the basic physical elements of the binary. To read Fig. 1 properly, please note that only Stebbins, *Hipparcos*, and Hvar observations are shown as individual observations, all others being either normal points or means of several consecutive observations. At Hvar, δ Orionis can only be observed at air masses of 1.4 and higher which contributes to the scatter (also seen in the observations of the check star 33 Ori). In spite of these shortcomings, the changing position of the secondary minimum due to apsidal motion is clearly seen.

3. Improved ephemeris including the apsidal advance

The collected and new photometric and spectroscopic material allows deriving the improved ephemeris for the system. We used two computer programs: `FOTEL` (Hadrava 1990, 2004a) and `PHOEBE` (Prša & Zwitter 2005a,b, 2006) which is a development of the well-known program `WD` of Wilson and Devinney (1971), further developed by Wilson (see, e.g. Wilson 2007).

We proceeded in the following way:

1. We used all published RVs, complemented by our measurements of red Ondřejov spectrograms, to derive a solution with `FOTEL`. The period and the rate of apsidal advance were included in the solution and individual systemic velocities were derived for individual datasets of Table 1. Using the rms errors of individual datasets from this first solution, we weighted the datasets by outer weights inversely proportional to the squares of these rms errors and derived the final `FOTEL` RV solution. This is given in Table 3.
2. Using `PHOEBE`, we derived an independent solution for all light curves, also allowing for the convergency of the period and the rate of apsidal advance. This solution is also given in Table 3 under the name `PHOEBE` LC. It shows that there is a fairly good mutual agreement between the elements from spectroscopy and photometry.
3. To derive the final ephemeris to be used, we therefore imported all RV measurements of the primary into `PHOEBE`. Note, however, that the available versions of the `WD` program (and `PHOEBE`) can only treat one single file of the radial velocities for each component. This is not suitable since individual RV datasets of δ Orionis have obviously different systemic velocities (cf., e.g., Fig. 10 in H02), probably because of different zero points of different observers. The expected variation in the systemic velocity as the binary orbits the common centre of gravity with the distant tertiary does not agree with the observed changes. (The probable time of the periastron is in the middle of the last century, and in that time the velocity change should be largest, but the observed velocity is nearly constant in that time.) For `PHOEBE`, we therefore used RVs with the individual systemic velocities (as derived in the final `FOTEL` solution) subtracted. This means that one has to fix a zero systemic velocity in `PHOEBE`. This solution, which gives the final ephemeris, is the solution denoted `PHOEBE` LC&RV in Table 3.

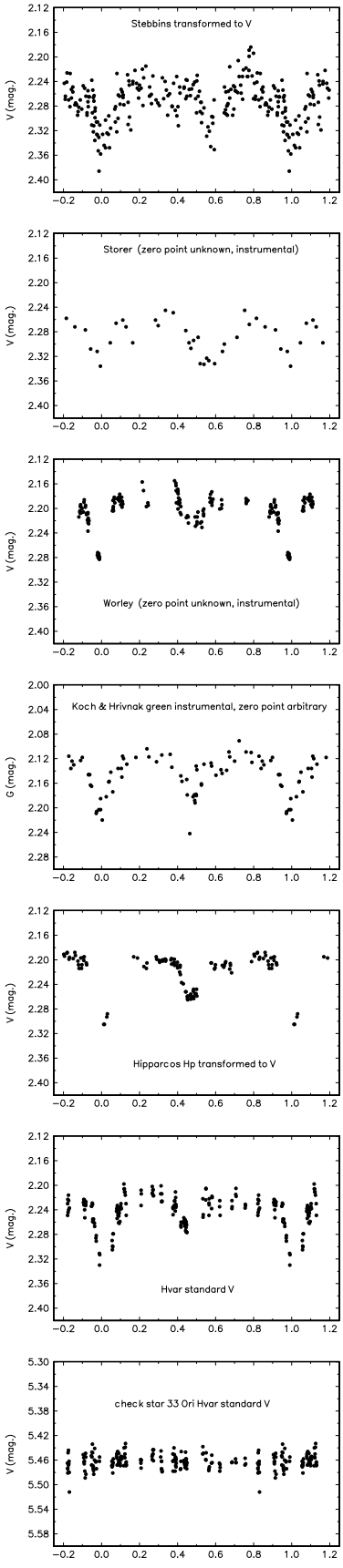

Fig. 1. Phase plots for individual homogenized data sets obtained in the visual region. Ephemeris used: Primary min.= JD 2 419 068.20 + $5^{\rm d}.732476 \times E$ (the ephemeris used by Koch & Hrivnak 1981, approximately valid for primary minima).

Table 3. Trial orbital and light-curve solutions aimed at determination of improved ephemeris for the binary.

Parameter	FOTEL RV	PHOEBE LC	PHOEBE LC&RV
$P_{\rm sidereal}$	$5^{\rm d}.732436(15)$	$5^{\rm d}.732436(3)$	$5^{\rm d}.732436(1)$
$P_{\rm anom}$	$5^{\rm d}.732824(15)$	$5^{\rm d}.732798(3)$	$5^{\rm d}.732821$
$T_{\rm periastr.}$	2.780(46)	2.7241(96)	2.7775(34)
$T_{\rm min.\,I}$	1.984	1.9641	1.9701
e	0.0910(37)	0.0858(41)	0.0883(26)
ω (°)	149.2(3.0)	145.6(3.9)	149.1(2.3)
$\dot{\omega}$ (°/d)	0.00425(16)	0.00397(29)	0.00422(11)
No. of obs.	824	635	824 + 635

Notes. The epochs of periastron passage are in HJD−2454000. The rms errors of the last two quoted digits are given in brackets after the respective values.

4. Towards true RV curves

Besides the Balmer and He I 6678 Å lines, He II lines are also present in the spectra of δ Ori: namely, the 6683 Å line is clearly visible at the red wing of the He I 6678 Å line. The C III 5695 Å line is in emission, as it is common among stars of O 9.5 spectral type and luminosity classes III and higher.

H02 concludes that three of their He I 6678 Å profiles were affected by some emission. Although our line profiles differ in their widths and depths, we found no evidence of emission in them. The differences are at the level of about ±6%, but changes of EWs are small. Variable emission/absorption is however present in Hα, as already discussed by Singh (1982). This is why we restrict this study to analysis of He lines.

When analysing the He I 6678 Å line, H02 applied the CCF method, as in the case of the IUE spectra. However, they are silent about the line of the tertiary, although its effect on the primary and secondary lines might be strong. Once again, we conclude the wings of the third line are probably responsible for the residuals in their Fig. 7.

To provide quantitative support for our alternative interpretation, we used two independent techniques:

- modelling the He I 6678 Å line profiles with Gaussians profiles properly shifted in RV;
- analysing them with the disentangling program KOREL (Hadrava 1995, 1997, 2004b).

4.1. Modelling the profiles with two Gaussians

The spectra taken during an interval shorter than 1 h were co-added for the purpose of this analysis. Our iterative procedure is illustrated in a series of diagrams that follows. The upper panel of Fig. 2 provides an example of the $\lambda\lambda$ 6678 & 6683 Å blend. The observed profile is fitted with two Gaussians for the primary contribution, the deeper for the He I 6678 Å line, the shallower for the He II 6683 Å line. The He II 6683 Å Gaussian has $FWHM$ = 6.5 Å and depth 0.015 of the continuum; with such values, one can fit all observed profiles (more accurate fitting see below). The $FWHM$ of the primary Gaussian varies from 3.7 to 4.6 Å, the depth from 0.099 to 0.128. For the profile shown in the upper panel, $FWHM$ = 4.12 Å, depth 0.114, RV = 117.9 km s^{-1}. In the case of a very positive velocity, the red wing of the profile is only formed by the primary He II line, without any contribution from the tertiary or secondary.

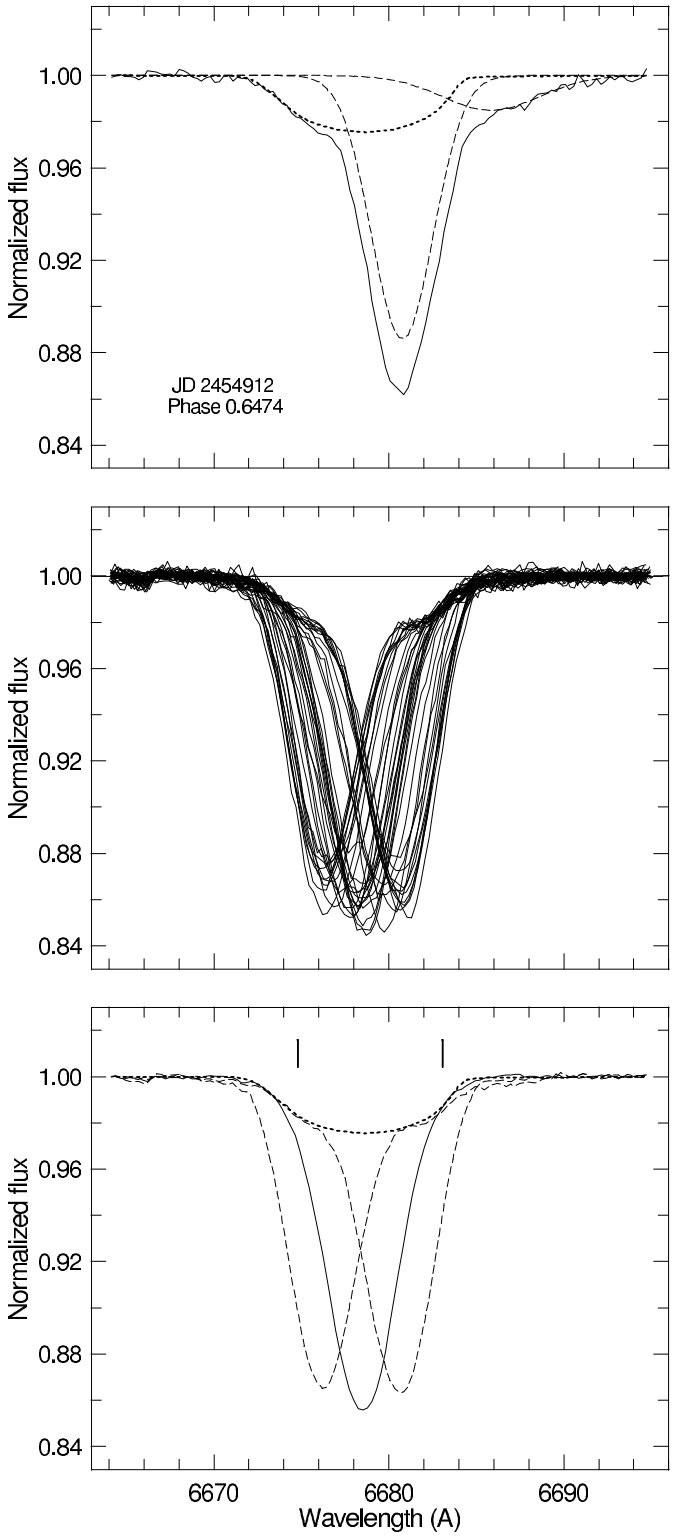

Fig. 2. *Upper panel*: an example of the observed profile (full line) with Gaussians for the He I and He II lines of the primary (dashed lines) and a broad, rotational profile for the third component (dotted line). *Central panel*: profiles of the observed spectra (He II feature subtracted); among them there is the space for the third line. *Bottom panel*: average profiles of quadratures and conjunction spectra (He II feature subtracted). The rotational profile of the third body is included.

To compare the profiles observed at various phases, we subtracted the He II 6683 Å line from them. These corrected profiles, with the exception of those having a low S/N, are plotted in the central panel of Fig. 2. Clearly, the third-line contribution (TC) has to be common to all profiles; i.e., TC might fill the free space between the plotted profiles. No other process can explain the upper parts of the profiles except the presence of another component.

The space is fitted well by a rotational profile from the OSTAR database (Lanz & Hubeny 2003) for $T_{\rm eff}$ = 30 000 K, $\log g$ = 4.00, $V_{\rm rot}$ = 240 km s^{-1}. The profile is shifted in RV to V = +25 km s^{-1} and reduced to 0.31 of its intensity.

The large width of TC agrees with the results of H02, but describes the contribution more accurately. It also excludes the possibility, mentioned by H02, that the third component itself could be a binary; the wings of the observed profiles at identical phases would have to vary, which is not the case.

It would, of course, be desirable to also identify the spectral line of the secondary. This line should be visible in the profiles taken at quadratures and invisible in profiles taken near conjunctions. Therefore, we formed three groups of observed profiles and calculated their averages: from spectra with RVs over 105 km s^{-1}, below −85 km s^{-1} and between +3 and +25 km s^{-1}. These averaged profiles are shown in the bottom panel of Fig. 2. The space for the secondary line is only between the quadrature profiles and the conjunction profile. But nothing is visible between these profiles in quadrature with a positive primary RV, and there is only a small space in the other quadrature. Certainly no large contribution from the secondary, comparable to what is advocated by H02, is acceptable (the expected positions of the secondary lines in quadratures are shown for K_2 = 186, V_γ = +35 km s^{-1}).

To understand the absorption in the red wings we subtracted the He I 6678 Å profile of the third body from the observed profiles. This profile is independent of the phase, but the He II 6683 Å profile might be phase dependent from the strong dependence of this line on temperature and gravity (see e.g. Lanz & Hubeny 2003). Figure 3 shows the profiles averaged for several phase intervals. Clearly, the profile for the quadrature with a positive primary RV agrees with the Gaussian profile we used in the former step. But an additional absorption is present in the quadrature with the negative primary RV. Its maximum is at 6683 Å, so this could be the He I 6678 Å line of the secondary with an RV of ∼220 km s^{-1}. However, a similar additional absorption, with an identical wavelength, is also seen in the conjunction profile; in any case, it would be strange if the secondary line was visible in only one quadrature.

A definitive answer can be given by the He II 6406.4 Å line, which is present in our spectra as a weak feature. This line is also strongly dependent on $T_{\rm eff}$ and $\log g$. Its profiles in both quadratures (obtained as sums of a dozen of observed spectra) presented in Fig. 4 display similar behaviour to He II 6683 Å: there is an additional absorption near zero velocity in the profile at the quadrature with the negative primary RV. As no such absorption is present at the opposite quadrature, this absorption cannot originate in the third body or in the secondary. However, to study it in more detail, more spectra of He II lines would be needed.

The measured Gaussian RVs of the primary are plotted in Fig. 5 and the corresponding orbital solution presented in Table 4; the rms per 1 RV observation is 4.1 km s^{-1}. The orbit was calculated again using the program FOTEL. The anomalistic period and the rate of periastron advance were kept fixed at values of $5\overset{\rm d}{.}732821$ and 0.00422 degrees per day. As could be expected, and as is known from other cases (see e.g. LY Aur, Popper 1982), when a TC is taken into account, the resulting

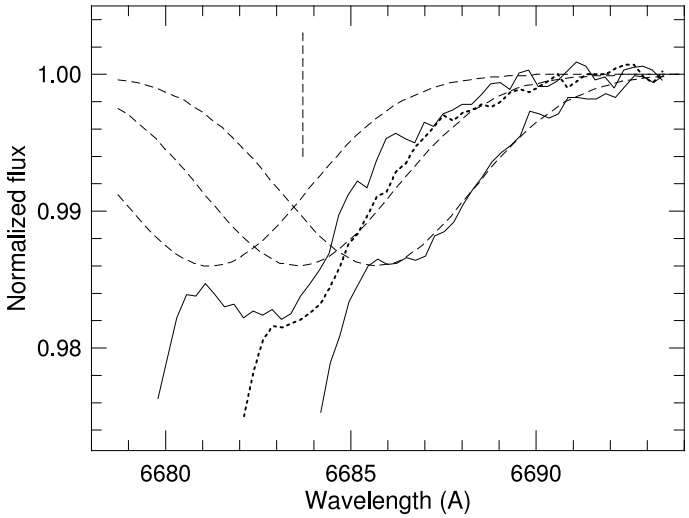

Fig. 3. The red wings of the observed He I 6678 Å profiles after subtracting the line profile of the third body. *From the left*: the profile at quadrature with the most negative primary RV (solid line), the profiles at conjunctions (dotted line), and the profile at quadrature with the most positive primary RV (full line). The dashed lines represent the corresponding contributions from the primary He II 6683 Å profile. The vertical dashed line is at V_γ.

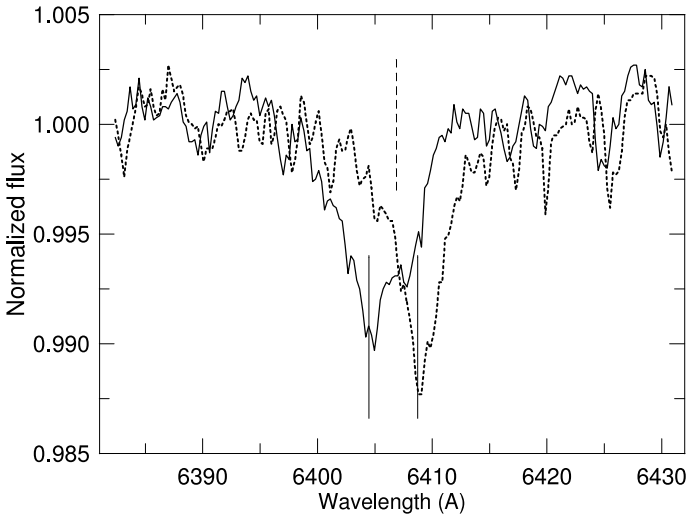

Fig. 4. Profile of the He II 6406 Å line in both quadratures. Full vertical lines denote the expected line positions corresponding to K_1 = 106.3 km s^{-1}, V_γ = 21.7 km s^{-1}; the dashed line is at V_γ.

semi-amplitude of the primary RV curve increases. In the previous studies of δ Orionis – including H02 – the effect of the third line on the primary RVs was not considered; therefore, our K_1 is larger than for all already published RVs.

4.2. Spectral disentangling

We used the program KOREL[1] developed by Hadrava (1995, 1997, 2004b) to the spectral disentangling. Preparation of data for the program KOREL deserves a few comments. The Ondřejov spectra have dispersion of 17.2 Å and are recorded with a wavelength step of 0.256 Å, which translates to an RV resolution of about 12 km s^{-1}. For investigation of the neighbourhood of

[1] The freely distributed version from Dec. 2004.

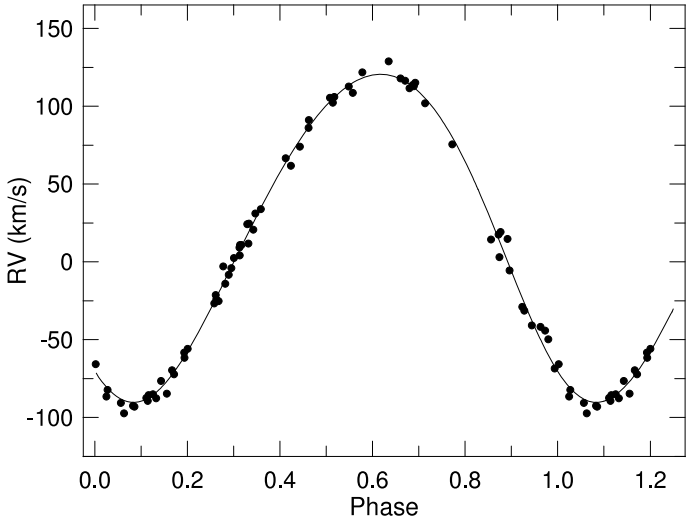

Fig. 5. Radial velocity curve of δ Orionis primary component. The curve corresponds to the solution given in Table 4.

Table 4. The orbital solution with FOTEL based on the Gaussian RVs of the primary.

Element	FOTEL /Gaussian RVs
$T_{\text{periastr.}}$ (HJD)	2 454 002.705 ± 0.060
e	0.0955 ± 0.0069
ω (°)	144.0 ± 3.9
K_1 (km s^{-1})	106.33 ± 0.71
V_γ (km s^{-1})	21.7 ± 0.5

the He I 6678 Å and He II 6406 Å, we oversampled the spectra, rebinning them with steps of 2.2 and 2.0 km s^{-1}, respectively. The rebinning was carried out with the help of the HEC35D program written by PH[2], which derives consecutive discrete wavelengths via

$$\lambda_{\text{n}} = \lambda_1 \left(1 + \frac{\triangle RV}{c}\right)^{\text{n}-1}, \quad (1)$$

where λ_1 is the chosen initial wavelength, $\triangle RV$ the constant step in RV between consecutive wavelengths, and λ_n the wavelength of the nth rebinned pixel. Relative fluxes for these new wavelength points are derived using INTEP (Hill 1982), which is a modification of the Hermite interpolation formula. It is possible to choose the initial and last wavelengths, and the program smoothly fills in the rebinned spectra with continuum values of 1.0 at both edges[3].

To take the variable quality of individual spectra into account, we measured their S/N in the line-free region 6630–6650 Å, and assigned each spectrum a weight according to formula

$$w = \frac{(S/N)^2}{(S/N_{\text{mean}})^2},$$

where S/N_{mean} denotes the mean S/N of all spectra. Specifically, the S/N ranged from 100 to 900, translating to the weights between 0.05 and 3.60.

[2] The program HEC35D with User's Manual is available to interested users at http://astro.troja.mff.cuni.cz/ftp/hec/HEC35

[3] This is necessary since KOREL requires that the number of the input data points is an integer multiple of 512.

Table 5. KOREL disentangling orbital solutions for the spectral regions near the He I 6678 Å line, and near the He II 6406 Å line.

Element	6665–6695 Å	6395–6416 Å
$T_{\rm periastr.}$	54 002.785	54 002.768
ω (°)	149.2	148.3
K_1(km s^{-1})	108.5	107.9

Notes. All epochs are in HJD-2400000.

We briefly recall that KOREL uses the observed spectra and derives both the orbital elements and the mean individual line profiles of the two binary components. Considering that some spectra were obtained during the eclipses and that the object also exhibits obvious physical line-strength variations, we allowed for variable strengths of the spectral lines in individual spectra during the solutions – cf. Hadrava (1997).

Our experience with KOREL is that the result is sensitive to the choice of starting values of the elements and initial values of the simplex steps. This is understandable since the sum of squares of residuals using all data points of individual spectra is a very complicated one, and it is easy to end up in a local minimum. This has been nicely illustrated in an excellent study of DW Car by Southworth & Clausen (2007) – see their Fig. 3. There is also another problem to complicate the task of finding the optimal elements. If – as is obviously the case for δ Orionis – the spectral lines of the secondary component are much fainter than those of the primary, their effect on the resulting sum of squares is very small. As a consequence, solutions for a wide range of mass ratios would appear as comparably good ones.

Before mapping the sum of residuals vs. trial values of the semiamplitude of the primary, we derived trial solutions, using the value of K_1 estimated from the Gaussian fits and adopting the astrometric solution of Mason et al. (2009) for the orbit of the tertiary. We investigated two useful spectral regions: the neighbourhood of the He I 6678 Å line and a close neighbourhood of the He II 6406 Å line. In these trial solutions, we allowed disentangling of both spectral regions into *three stellar components*. We obtained straight lines at continuum for both the disentangled secondary in the two regions and the tertiary in the He II 6406 Å line region. In other words, no lines of the secondary and the He 6406 line of the tertiary could be detected above the detection treshold of some 0.003 of the continuum level. For that reason, we did the final parameter space mapping for the primary and tertiary only for He I 6678 Å, and for the primary and the telluric spectrum for the neighbourhood of the He II 6406 Å line. The plot of the sum of squares of residuals as a function of the semi-amplitude K_1 is shown in Fig. 6, separately for the He I 6678 Å and He II 6406 Å line. One can see that the variation is not quite smooth but that it clearly identifies the most probable semi-amplitude of the primary near some 107 km s^{-1}, in good agreement with the result based on the Gaussian fits.

We then derived a number of trial solutions where we only kept the anomalistic period ($5^{\rm d}.732821$), apsidal advance (0.00422 degrees per day) and eccentricity fixed, and starting with K_1 near 107 km s^{-1}. The final KOREL solutions for both lines, giving the smallest sums of residuals, are in Table 5. Renormalizing the continua of disentangled spectra according to the light-curve solution (see the next section), we obtained the final line profiles shown in Fig. 7.

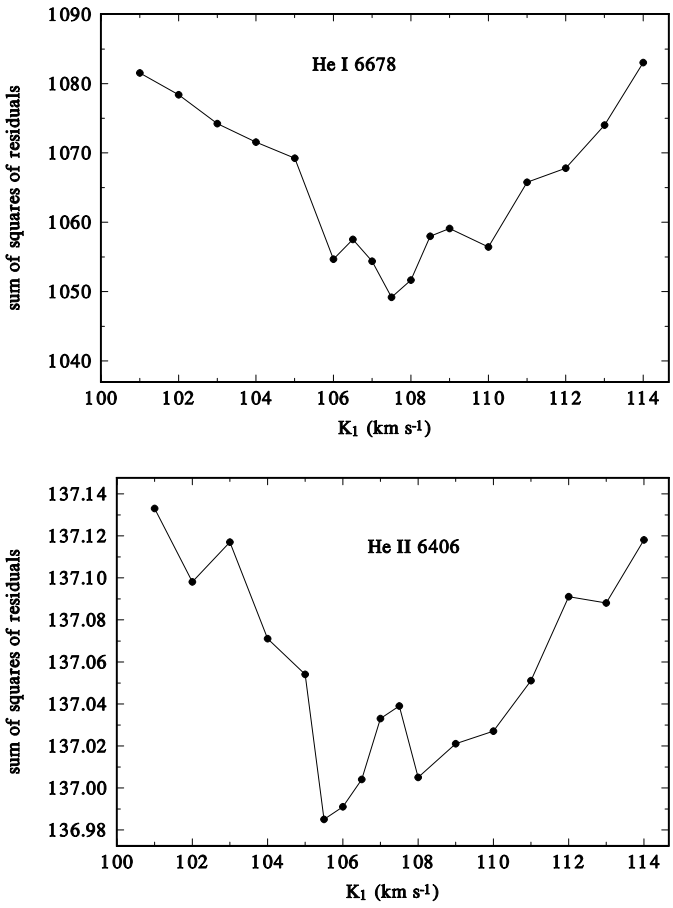

Fig. 6. The sum of squares of residuals of exploratory KOREL solutions as a function of the semiamplitude of the primary K_1 for the He II 6678 Å and He II 6406 Å lines. See the text for details.

5. Light-curve solution

Keeping the orbital period, the rate of apsidal advance, and eccentricity fixed at the values from the last solution of Table 3, we derived the final combined solution with PHOEBE, using all available photometry and the Gaussian RVs for the primary. The $T_{\rm eff}$ of the primary was kept fixed at 30 000 K because it follows, e.g., from the calibration by Martins et al. (2005). We also assumed that the third light contributed 21.6% in all passbands and used linear limb darkening coefficients. The anomalistic period and the rate of periastron advance were kept fixed at values of $5^{\rm d}.732821$ and 0.00422 degrees per day. Since we were unable to find any spectral lines of the secondary, we had to assume something. We decided to adopt a reasonable mass of 25 $M_\odot$ for the primary.

The solution with a free convergency (solution I) of all elements gave results that did not agree with expectations – the primary radius was too small. As a consequence, the absolute visual magnitude and the resulting distance were small. Also the effective temperature of the secondary T_2 was under 20 000 K, although temperature of a young 10 $M_\odot$ star should be about 24 000 K. Therefore, we derived other solutions with the effective temperature of the secondary fixed at 24 000 K. In solution II, we moreover fixed the relative radius of the primary, while in solution III the relative radius of the secondary was fixed. During solutions, we tuned the mass ratio q to fit the known mass function $f(m) = 0.71$ and the inclination as it followed from the solution. The mass ratio was always between

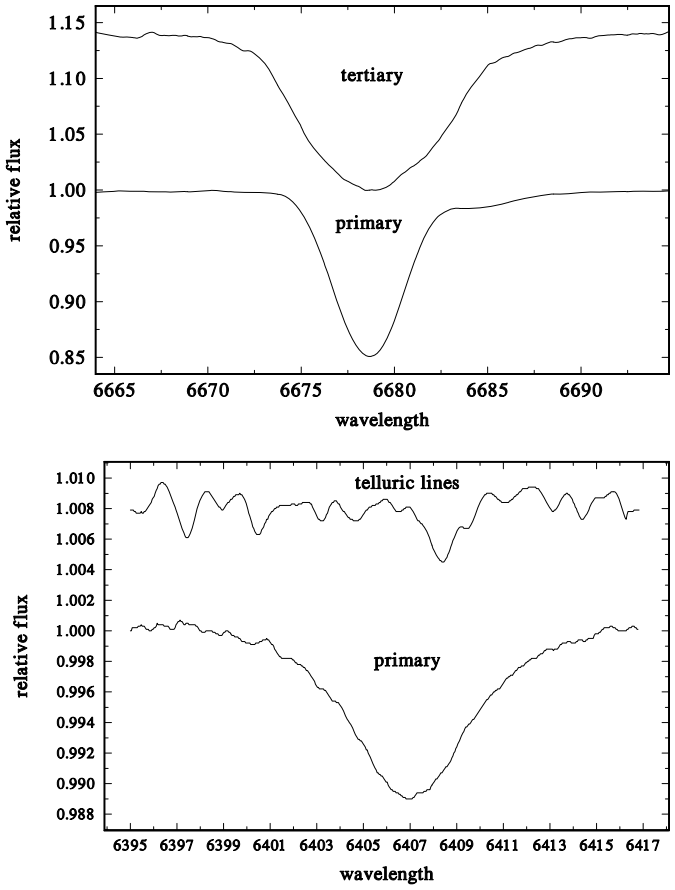

Fig. 7. The line profiles disentangled by KOREL and normalized to their individual continua according to the light-curve solutions ($L_1 = 0.755$, $L_3 = 0.216$). *Upper panel*: the He I 6678 Å and He II 6683 Å line profiles of the tertiary and primary. *Bottom panel*: the telluric spectrum and the He II 6406 Å line profile of the primary. In both panels, the spectra were shifted in flux for clarity, and there are very different flux scales in the two panels.

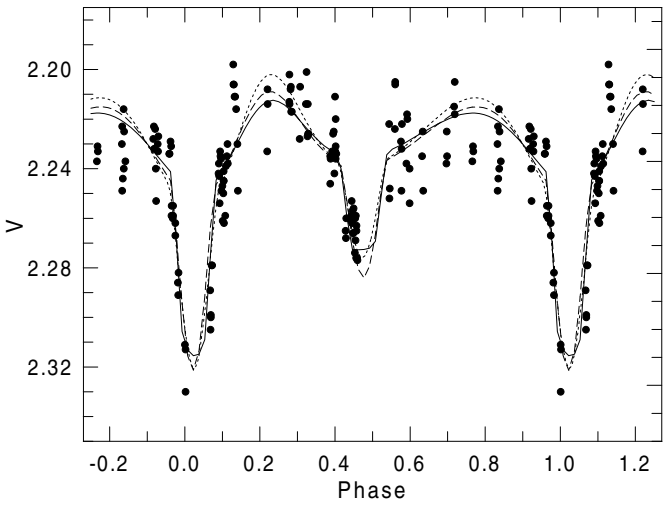

Fig. 8. Hvar V measurements compared with PHOEBE solutions: I – full curve, II – short-dash curve, III – long-dash curve.

0.38 and 0.42, i.e., $M_2 \approx 10\ M_\odot$. Our results are summarized in Table 6.

In the latest (development) version of PHOEBE that we are using, the convergency is governed by minimalization of a cost function χ defined in the case of our datasets as

$$\chi^2 = \sum_p \frac{1}{\sigma_p^2} \sum_{i=1}^{N_p} w_i (f_i - s_i)^2, \qquad (2)$$

where index p denotes the individual photometric passbands, σ_p their standard deviations per 1 observation, N_p is the number of individual observations for pth passband, w_i are standard weights of individual observations, and f_i and s_i are the observed and calculated fluxes, respectively.

The cost function for both constrained solutions is naturally a bit higher, but the comparison of the resulting model V light curves with the observed Hvar V light curve, presented in Fig. 8, shows that all these solutions fit the observed curve within the limits of its scatter (all photometry was used to obtain the solutions, but owing to apside line advance, only observations from a limited time interval are shown). In other words, one must conclude that a whole class of possible solutions is tolerable with the light curves at hand. When H02 solved the *Hipparcos* light curve, their result also was that a wide interval of solutions is possible. Their radii of the primary 9 and 13 $R_\odot$ (obtained for $a = 34.5\ R_\odot$) can be transformed for our $a \approx 44\ R_\odot$ to 11.5 and 16.6 $R_\odot$. In spite of including several times more numerous data, our results are similar.

Parameters that would follow from the system's membership in the Orion complex are therefore allowed. The membership means that the primary M_V is about $-5\overset{m}{.}7$. The M_V of the three-body system is then $-6\overset{m}{.}0$ and with the magnitude at maximum $V = 2\overset{m}{.}20$ and interstellar absorption $A_V = 0.20$ the distance moduli is 8.0, comparable e.g. to the distance 413 pc of Trapezium (Menten et al. 2007). With the radius R_{pri} about 17 $R_\odot$, the age of the primary is ≈5.5 My (Claret 2004); the secondary component is very probably a star of identical age. With the mass ≈10 $M_\odot$, its radius should be about 4.3 $R_\odot$ and temperature 24 000 K. Even with $r_1 = 0.38$ the primary is well inside Roche lobe: its volume equals about 57% of the Roche lobe volume as calculated using the formula by Eggleton (1983).

6. Discussion

In this paper, several arguments are given against detection of secondary absorption lines by H02 in δ Orionis . It is mainly the unreliability of the CCF results – very probably, CCFs obtained by H02 contain information on the third line, not on the secondary. When disentangling He I 6678 Å line, H02 did not *find* the secondary line, only *assumed* it. Therefore, the component masses found by H02 cannot be trusted.

According to the BSTAR spectra (Lanz & Hubeny 2007), theoretical equivalent widths of the He I 6678 Å line are ≈0.50 Å in the primary, as well as in the secondary component. Then the observed width of the primary line should be 0.38 Å. (But the real observed width is 0.47 Å; such deviations are known for other high-luminosity stars, too). Under assumptions of "normality" for both binary components, the secondary is 26-times weaker in V, and its observed line should have $EW = 0.015$ Å. If the components rotate synchronously, the secondary $FWHM$ is about 1.5 Å, therefore the line depth would be 0.01 of the continuum. No such lines are visible in Figs. 2 (bottom) or 3; the limit for the detection is several times smaller, i.e., the secondary He I 6678 Å line is several times weaker than it should be.

Therefore, instead of the problem of very low masses, we are confronted with another problem – very small EW of the

Table 6. The final combined solution with PHOEBE, based on all photometric data sets and Gaussian RVs for the primary.

Element	Solution I	Solution II	Solution III
$T_{\mathrm{min.I}}$	54 001.9787 ± 0.0040	54 001.9657 ± 0.0044	54 001.9635 ± 0.0041
a ($R_\odot$)	43.9 ± 0.3	44.2 ± 0.3	44.0 ± 0.3
V_γ (km s^{-1})	21.74 ± 0.50	21.77 ± 0.51	21.74 ± 0.50
ω (deg)	148.7 ± 2.4	144.2 ± 2.1	140.0 ± 1.8
i	81.°0 ± 1.°1	67.°6 ± 0.°4	73.°6 ± 0.3
$q = M_2/M_1$	0.3821	0.4147	0.3962
Ω_1	3.534 ± 0.055	3.156 (given by r_1)	3.328 ± 0.034
Ω_2	5.615 ± 0.084	4.008 ± 0.081	5.065 (given by r_2)
r_1	0.326	0.380 (fixed)	0.353
r_2	0.091	0.158	0.108 (fixed)
$T_{\mathrm{eff.1}}$ (K)	30 000 (fixed)	30 000 (fixed)	30 000 (fixed)
$T_{\mathrm{eff.2}}$ (K)	19 380 ± 520	24 000 (fixed)	24 000 (fixed)
L_1 Johnson V	0.7556 ± 0.0019	0.6986 ± 0.0054	0.7355 ± 0.0021
L_1 Johnson B	0.7578 ± 0.0021	0.7015 ± 0.0054	0.7372 ± 0.0023
L_1 Johnson U	0.7599 ± 0.0018	0.7043 ± 0.0052	0.7389 ± 0.0019
L_2 Johnson V	0.0284	0.1010	0.0485
L_2 Johnson B	0.0262	0.0825	0.0468
L_2 Johnson U	0.0241	0.0797	0.0451
M_1 ($M_\odot$)	25.0 (adopted)	25.0 (adopted)	25.0 (adopted)
M_2 ($M_\odot$)	9.55	10.4	9.91
R_1 ($R_\odot$)	14.3	16.8	15.6
R_2 ($R_\odot$)	4.0	7.0	4.8
M_{bol1}	$-8^{\mathrm{m}}.19$	$-8^{\mathrm{m}}.54$	$-8^{\mathrm{m}}.37$
M_{bol2}	$-3^{\mathrm{m}}.52$	$-5^{\mathrm{m}}.67$	$-4^{\mathrm{m}}.83$
log g_1 [cgs]	3.52	3.38	3.45
log g_2 [cgs]	4.22	3.76	4.08
cost function χ	1006.3	1089.9	1064.1

secondary He I 6678 Å line. We do not have any explanation; however, we can say that a very similar situation was met by Popper (1993) in his discussion of the spectra of V1765 Cyg. This binary bears some similarity to δ Ori: the spectral type is B 0.5 Ib, the orbit is eccentric, and $L_{\mathrm{V},1}/L_{\mathrm{V},2} = 12$; the period is $13^{\mathrm{d}}.4$. Popper did not find the secondary line He I 5786 Å and estimated that it is 35 times or more weaker than the primary line, i.e. several times weaker than it should be, the problem identical to the case of He I 6678 Å in δ Ori.

Because it is $1^{\mathrm{m}}.4$ fainter than the primary, the third body should be of about O 9 IV type, with $T_{\mathrm{eff}} \approx 32\,000$ K. In spite of this high temperature, the He II 6683 Å and 6406 Å lines are not expected to be present as both strongly depend on gravity. Naturally, it would be helpful if a separated spectrum of the visual component could be acquired, for example using adaptive optics.

It is known that there are systems where the lines of their seconaries are invisible presumably due to circumstellar envelopes, but they possess longer periods (HD 187399, $P = 28$ d, $e = 0.39$) or circular orbits. In this connection, please note that the suggestion by H02 that the eccentricity might stem from the visual component is not acceptable, because the time scale of any such effect is about 10^{10} years, see Eggleton & Kiseleva-Eggleton (2001). Also the effect of the third body on the apside line rotation might only be small – according to Söderhjelm (1981), the apside line period would be 10^7 years if its only reason was the third body.

Acknowledgements. We gratefully acknowledge the use of spectrograms of δ Orionis from the public archives of the Elodie spectrograph of the Haute Provence Observatory. Some of the Ondrejov spectrograms were obtained by Drs. M. Dovčiak, P. Hadrava, M. Kraus, J. Kubát, V. Šimon, and P. Škoda, Ms. B. Kučerová and Messrs. M. Ceniga and M. Netolický. Drs. D. Ruždjak and D. Sudar helped with photometry at the Hvar Observatory. Comments and suggestions by an anonymous referee helped to improve the structure and argumentation of this paper. This study was supported from the grants 205/06/0304, 205/06/0584, and P209/10/0715 of the Czech Science Foundation and also from the research plan J13/98: 113200004 of the Ministry of Education, Youth and Sports *Investigation of the Earth and Universe*, and later also from the Research Programme MSM0021620860 *Physical study of objects and processes in the solar system and in astrophysics* of the Ministry of Education of the Czech Republic. We acknowledge the use of the electronic bibliography maintained by NASA/ADS system and by the CDS in Strasbourg.

References

Campbell, W. W. 1901, PASP, 13, 162
Campbell, W. W., & Moore, J. H. 1928, Publ. Lick Obs., 16, 74
Claret, A. 2004, A&A, 424, 919
Curtiss, R. H. 1915, Publ. Michigan, 1, 118
Deslandres, H. 1900a, Comptes Rendus, 130, 379
Deslandres, H. 1900b, Observatory, 23, 148
Deslandres, H. 1904, AN, 166, 33
Eggleton, P. P. 1983, ApJ, 268, 368
Eggleton, P. P., & Kiseleva-Eggleton, L. 2001, ApJ, 562, 1012
Hadrava, P. 1990, Contr. Astron. Obs. Skalnaté Pleso, 20, 23
Hadrava, P. 1995, A&AS, 114, 393
Hadrava, P. 1997, A&AS, 122, 581
Hadrava, P. 2004a, Publ. Astr. Inst. Acad. Sci. Czech Rep., 89, 1
Hadrava, P. 2004b, Publ. Astr. Inst. Acad. Sci. Czech Rep., 89, 15
Harmanec, P. 1998, A&A, 335, 173
Harmanec, P., & Božić, H. 2001, A&A, 369, 1140
Harmanec, P., & Horn, J. 1998, J. Astron. Data, 4, file 5
Harmanec, P., Horn, J., & Juza, K. 1994, A&AS, 104, 121
Harries, T. J., Hilditch, R. W., & Hill, G. 1998, MNRAS, 295, 386
Hartmann, J. 1904, ApJ, 19, 268
Harvey, A. S., Stickland, D. J., Howarth, I. D., & Zuiderwijk, E. J. 1987, Observatory, 107, 205
Harvin, J. A., & Gies, D. R. 2002, in Exotic Stars as Challenges to Evolution, ed. C. A. Tout, & W. van Hamme, ASP Conf. Ser., 279, 47
Harvin, J. A., Gies, D. R., Bagnuolo, W. G., Penny, L. R., & Thaller, M. 2002, ApJ, 565, 1216
Heap, S. R., Lanz, T., & Hubeny, I. 2006, ApJ, 638, 409
Heintz, W. D. 1980, ApJS, 44, 111
Hill, G. 1982, Publ. Dominion Astrophys. Obs., 16, 67
Hillier, D. J., & Miller, D. L. 1998, ApJ, 496, 407
Hnatek, A. 1921, AN, 213, 17

Holmgren, D. E., Hadrava, P., Harmanec, P., et al. 1999, A&A, 345, 855
Horch, E., Ninkov, Z., & Franz, O. G. 2001, AJ, 121, 1583
Horn, J., Kubát, J., Harmanec, P., et al. 1996, A&A, 309, 521
Johnson, H. L., Iriarte, B., Mitchell, R. I., & Wisniewski, W. Z. 1966, CoLPL, 4, 99
Jordan, F. C. 1916, Publ. Allegheny Obs., 3, 125
Koch, R. H., & Hrivnak, B. J. 1981, ApJ, 248, 249
Lanz, T., & Hubeny, I. 2003, ApJS, 146, 417
Lanz, T., & Hubeny, I. 2007, ApJS, 169, 83
Luyten, W. J., Struve, O., & Morgan, W. W. 1939, Publ. Yerkes Obs., 7, 256
Martins, F., Schaerer, D., & Hillier, D. J. 2005, A&A, 436, 1049
Mason, B. D., Martin, C., Hartkopf, W. I., Barry, D. J., Germain, M. E., et al. 1999, AJ, 117, 1890
Mason, B. D., Hartkopf, W. I., Gies, D. R., Henry, T. J., & Helsel, J. W. 2009, AJ, 137, 3358
Menten, K. M., Reid, M. J., Forbrich, J., & Brunthaler, A. 2007, A&A, 474, 515
Miczaika, G. R. 1952, ZfA, 30, 299
Moultaka, J., Ilovaiski, S. A., Pruguiel, P., & Soubiran, C. 2004, PASP, 116, 693
Natarajan, V., & Rajamohan, R. 1971, KodOB, 208, 219
Perryman, M. A. C., & ESA 1997, The Hipparcos & Tycho Catalogues, ESA SP–1200
Pişmiş, P., Haro, G., & Struve, O. 1950, ApJ, 111, 509
Penny, L. R., Seyle, D., Gies, D. R., et al. 2001, ApJ, 575, 1050
Popper, D. M. 1982, ApJ, 262, 641
Popper, D. M. 1953, PASP, 105, 721
Prša, A., & Zwitter, T. 2005a, ApJ, 628, 426
Prša, A., & Zwitter, T. 2005b, ESA SP-576, 611
Prša, A., & Zwitter, T. 2006, Ap&SS, 304, 347
Schmidt-Kaler, Th. 1982, in Landolt-Börnstein, 2b (Berlin: Springer), 453
Singh, M. 1982, Ap&SS, 87, 269
Skoberla, P. 1935, ZfA, 11, 1
Škoda, P. 1996, in Astronomical Data Analysis Software and Systems V, ASP Conf. Ser., 101, 187
Söderhjelm, S. 1981, A&A, 42, 229
Southworth, J., & Clausen, J. V. 2007, A&A, 461, 1077
Stebbins, J. 1915, ApJ, 42, 133
Stebbins, J. 1911, ApJ, 34, 105
Storer, N. W. 1930, PASP, 42, 291
Vogel, H. C., & Scheiner, J. 1892, Publ. Astrophys. Obs. Potsdam, 7, Part I, 100
Wilson, R. E. 2007, in IAU Symp. 240, ed. by W.I. Hartkopf, E.F. Guinan, & P. Harmanec (Cambridge Univ. Press), 188
Wilson, R. E., & Devinney, E. J. 1971, ApJ, 166, 605
Walborn, N. L. 1972, AJ, 77, 312
Worley, C. E. 1955, PASP, 67, 330

Pages 10 to 12 are available in the electronic edition of the journal at http://www.aanda.org

Appendix A: Overview of available RV observations

We reduced and measured two sets of electronic spectra secured at the coudé focus of the 2-m reflector of the Ondřejov Observatory which cover the red spectral region containing the Hα and He I 6678 Å lines. These spectra have a linear dispersion of 17.2 Å mm^{-1} and a 2-pixel resolution of 12 700 (11–12 km s^{-1} per pixel).

1. In the period 1993–2000, 20 spectra were obtained with a Reticon 1872RF linear detector. They cover the wavelengths from 6305 to 6740 Å and have the S/N between 110 and 900.
2. A series of 204 spectrograms obtained with a SITe-005 800× 2000 CCD detector secured between 2003 and 2010. They cover a slighly longer wavelength region 6255–6765 Å and have S/N between 200 and 880.

There are also four echelle spectra publicly available in the ELODIE archive (Moultaka et al. 2004), which cover the interval from 4000 to 6700 Å. We consulted these spectra but have not used them for RV measurements because of their insufficient number and phase distribution.

The initial reductions of spectra were performed using the IRAF (Ondřejov CCD spectra and SPEFO (Ondřejov Reticon spectra) programs. All subsequent reductions and the RV measurements were carried out using the SPEFO reduction program written by the late Dr. J. Horn and then further developed by Dr. P. Škoda and by (now also late) Mr. J. Krpata (Horn et al. 1996; Škoda 1996). Note that SPEFO displays direct and reverse traces of the line profiles superimposed on the computer screen, and the user can slide them to achieve their exact ovelapping for the studied detail of the profile.

A.1. Radial-velocity data files

We carried out a critical compilation of all available RV measurements from the literature with the known dates of observations. In all cases where the original sources give the dates and times of mid-exposures, we used the program HEC19 to derive heliocentric Julian dates[4]. The journal of all RVs used in this study is in Table A.1.

When the number of measured lines N used to derive the mean RV was given in the original study, we applied internal weighting of individual RVs, assigning weights $w = 0.1 * N$. The only exception are Vienna RVs based on the mean of 11–38 individual lines. Here we used a linear transformation from the interval (11, 38) to (0.5, 1.5).

Comments on some individual files follow:

– *Spg. 1: Potsdam* Four very first RVs of δ Orionis were obtained by Vogel & Scheiner (1892) in 1888–1891 and showed no evidence of RV changes. They are based on RV of Hγ alone. When Deslandres (1900a) discovered the RV variations, Prof. Vogel remeasured the old spectra at the request of Dr. Hartmann. He found out that the last two spectra do show significant RV changes. His revised RVs are published in Hartmann's (1904) paper and should be preferred over the original measurements so are used by us.
– *Spg. 2: Meudon* Deslandres (1900a,b) published his discovery RVs giving only the days of observations. Hartmann (1904) republished his RVs with estimated fractions of the days of observations, but later Deslandres (1904) published the actual mid-exposure times of his observations and these are used by us.
– *Spg. 3: Lick* Three RVs from 1900 Lick spectra taken with the Mills pectrograph were obtained and measured by Dr. Wright and published by Campbell (1901), again without accurate mid-exposure times. Hartmann (1904) also estimated the times of mid-exposures for these spectra but we use the actual mid-exposure times published by Campbell & Moore (1928), adopting also mean RV from two independent measurements of these spectra for this last publication.
– *Spg. 6: Vienna* Hnatek (1921) tabulated mid-exposure times in Central European Mean Time (G.M.T.+1 h) and used this time also for the fractions of his Julian days. We derived and used correct HJDs.
– *Spg. 11: IUE* Harvey et al. (1987) analysed the first 44 SWP spectra obtained by the IUE. Their RV measurements were relative and the RVs published in their Table 1 have the zero point artificially shifted in such a way as to give the systemic velocity of 20.4 km s^{-1}, adopted from the study by Curtiss (1915). Harvin et al. (2002) later analysed the complete set of 60 IUE SWP spectra from the final IUE reduction. The derived RVs via cross-correlation, using the spectra of O 9.5V star AB Aur (HD 34078) as a template. Here we adopted their RVs.
– *Spg. 14&15: Kitt Peak and Mt. Stromlo* These RVs are solely based on the He I 6678 Å line and were also derived via cross-correlation by Harvin et al. (2002).
– *Spg. 13&16: Ondřejov* These RVs are also solely based on the He I 6678 Å line measured in SPEFO via comparison of direct and flipped line profile on the computer screen.

[4] This program, which handles data in various forms, together with brief instructions on how to use it, is freely available on the anonymous ftp server at http://astro.troja.mff.cuni.cz/ftp/hec/HEC19.

Appendix B: Photometry

After the discovery that δ Orionis is an eclipsing variable by Stebbins (1911, 1915), the binary was measured by several authors: Storer (1930), Skoberla (1935; only times of minima), Worley (1955, who also published measurements by Storer), and Koch & Hrivnak (1981). Then there is the photometry by *Hipparcos*.

We obtained new *UBV* observations using the automated photoelectric photometer attached to the 0.65-m reflector of the Hvar Observatory. The data were transformed to the standard *UBV* system via non-linear transformation (see Harmanec et al. 1994, for details).

The reductions were carried out with the latest version 16.1 of the HEC22 program (Harmanec & Horn 1998), which permits extinction variations to be modelled in the course of the night. To be able to also transform the old Stebbins (1915) photometry to the V magnitude, we also observed his comparison star ε Ori regularly during the first season.

The new observations were combined with several existing photometric data sets that we critically compiled from the literature. Basic information about all data sets used is summarized in Table B.1. Table B.2 summarizes the *UBV* magnitudes of all comparison stars used by different observers. Hvar mean all-sky magnitudes were added to all magnitude differences δ Orionis – comparison whenever these differences were known.

A few comments on individual data sets follow:

– Stebbins (1915): magnitude differences δ Orionis – ϵ Ori, secured with the Lick 12-inch refractor, were transformed to

Table A.1. Journal of available RV observations.

Spg. No.	Time interval (HJD−2400000)	No. of RVs	Telescope/ Instrument	Source
1	10 982.4–16 189.3	46	Potsdam 0.80-m refractor	Hartmann (1904)
2	14 997.5–15 045.4	11	Meudon 0.62-m refractor	Deslandres (1900a,1904)
3	15 245.0–15 281.0	3	Lick Mills	Campbell & Moore (1928)
4	18 297.7–19 479.6	36	Allegheny 0.76-m refractor	Jordan (1916)
5	19 474.6–20 236.6	74	Ann Arbor 0.95-m prism spg.	Curtiss (1915)
6	22 363.2–22 410.3	17	Vienna 0.30-m coudé	Hnatek (1921)
7	28 056.9–28 992.6	140	Yerkes 1.02-m, Bruce prism spg.	Luyten et al. (1939)
8	32 514.6–32 557.9	48	McDonald 2.08-m reflector	Pişmiş et al. (1950)
9	33 560.6–33 762.3	73	Heidelberg 0.72-m, prism spg.	Miczaika (1952)
10	40 216.6–40 655.2	49	Kodaikanal 0.50-m Cassegrain reflector	Natarajan & Rajamohan (1971)
11	43 753.5–48 546.9	60	International Ultraviolet explorer SWP spectra	Harvin et al. (2002)
12	44 654.9–44 950.2	23	Kavalur 0.50-m Cassegrain reflector	Singh (1982)
13	49 255.6–51 602.3	20	Ondřejov 2.0-m, grating spg.	this paper: Reticon spectra
14	49 613.0–49 617.9	6	Kitt Peak 0.91-m coudé feed spg.	Harvin et al. (2002)
15	50 150.9–50 537.9	14	Mount Stromlo 1.88-m reflector	Harvin et al. (2002)
16	52 957.5–55 293.3	204	Ondřejov 2.0-m, grating spg.	this paper: CCD spectra

Table B.1. Photometric data sets used.

Source	Time interval (JD-2 400 000)	No. of obs.	Comparison	Check	Passband(s)
Stebbins (1915)	18 681.7–19 309.9	191	HD 37128	–	green (V)
Storer (1930)	see the text	30	HD 35411	–	?
Worley (1955)	see the text	112	?	–	BV
Johnson et al. (1966)	38 304.0–38 729.9	5	all-sky	–	UBV
Koch & Hrivnak (1981)	43 865.7–44 326.5	64	HD 36840	HD 36898	green
	43 870.7–44 326.5	62	HD 36840	HD 36898	blue
Perryman et al. (1997)	47 915.7–49 061.5	89	all-sky	–	$H_p(V)$
this paper, Hvar	54 015.6–54 720.6	145	HD 36591	HD 36351	UBV

Table B.2. Comparison and check stars used by various photometric observers.

Name	HD	V	$B-V$	$U-B$	Source
ϵ Ori	37128	$1^m.69$	$-0^m.18$	−1.03	Johnson et al. (1966)
		$1^m.695 \pm 0^m.019$	$-0^m.180$	$-1^m.016$	Hvar all-sky
HR 1861	36591	$5^m.343 \pm 0^m.008$	$-0^m.188$	$-0^m.925$	Hvar all-sky
33 Ori	36351	$5^m.462 \pm 0^m.008$	$-0^m.180$	$-0^m.829$	Hvar all-sky
HIP 26149	36840	$6^m.251$	$0^m.986$	?	Simbad

Johnson V following Holmgren et al. (1999) and Harmanec & Božić (2001). The mean Hvar all-sky V magnitude of ϵ Ori, $1^m.695 \pm 0^m.019$ was then added to the transformed magnitude differences to get Stebbins' observations on the standard Johnson V magnitude. Note, however, that ϵ Ori is a known variable star (see Fig. B.1), so these early data must be treated with some caution.

– Storer (1930) and Worley (1955): Both these authors published their observations only in a graphical form. Their observations were also secured with the Lick 12-inch refractor, but no details about the photometer used by Storer are known. Worley used an EMI 5659 photomultiplier and Corning filters 3385 and 5543, which very closely match the B and V magnitudes of the Johnson system. He obtained about 300 yellow and 250 blue observations and formed 112 running means of them. Storer observed in the years 1926–1928 relative to η Ori ($V = 3^m.36$) and only showed plots of magnitude differences from several observed eclipses. They range from about $0^m.1$ to $0^m.2$; apparently the integral parts of the ordinate scale of his plot should be −1 instead zero. Worley (1955) obtained Storer's individual observations but he published them along with his own observations only in the form of a phase diagram, forming the normal points from the original Storer's observations. We therefore reconstructed these two sets of observations from his plot and assigned them "artificial" Julian dates corresponding to the mean times of observations of the respective data sets applying the ephemeris that Worley probably used: HJD 2419068.20 + $5^d.732476 \times E$[5]. This ephemeris is still close to the present ephemeris for the primary minimum. For the data by Storer (1930) and Worley (1955), the magnitude zero point is unknown, because Worley regrettably did not mention which comparison star he used. Since the colours of the comparison stars that were probably used are quite similar to those of δ Ori, we treat these data as yellow magnitudes in the photometric solutions.

[5] This value of the sidereal period is quoted by him and later also used by Koch & Hrivnak (1981), while the epoch had already been derived by Stebbins (1915) and used in subsequent studies.

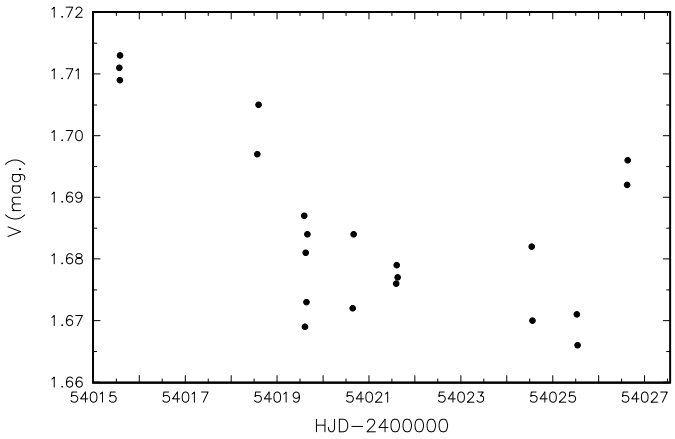

Fig. B.1. A time plot of the Hvar V observations of ε Ori, the star used as the comparison by Stebbins. Mild light variations are clearly seen.

- Johnson et al. (1966): we derived heliocentric Julian dates for these standard all-sky *UBV* observations.
- Koch & Hrivnak (1981): these authors obtained about 350 individual observations using a photoelectric photometer with an RCA 4509 tube attached to the 0.38-m refractor of the Flower and Cook Observatory and green and blue filters; however, they only published magnitude differences for 64 green and 62 blue normal points. We converted their JDs to HJDs again. The primary comparison they used, HD 36840 = HIP 26149, is a seldom studied G5 star ($V \sim = 6^{\rm m}.25$), and we found no way how to transform their observations to the Johnson V and B magnitudes. We therefore simply added estimated green and blue magnitudes of HD 36840, $6^{\rm m}.53$, and $7^{\rm m}.15$ to the published magnitude differences.
- Perryman & ESA (1997) These *Hipparcos* $H_{\rm p}$ observations were transformed to the standard V magnitude following Harmanec (1998) and assuming the mean all-sky Hvar colour indices for δ Ori: $B-V = -0^{\rm m}.219$, and $U-B = -1^{\rm m}.040$.

As a quality check, it is also useful to add a few comments on possible light variations on other time scales. All photometric observers of δ Orionis have concluded that the object is exhibiting cycle-to-cycle and, possibly also, hour-to-hour changes. The inspection of Fig. 1 indeed reveals a rather large scatter in virtually all visual light curves, although most of them are based on averaged data. A word of caution is appropriate, however, because Stebbins' and Storer's (if not also Worley's) observations were obtained using mildly variable comparison stars. As Hvar observations show, the scatter outside minima is comparable to what is observed for the check star and can to some extent be attributed to the fact that the star could only be observed at relatively high air masses.

What can be suspected, however, is the different height of the maxima between the two eclipses, which might also vary secularly. Only more systematic observations from a good site can decide whether it is indeed so.